ARCETRI-ADOPT
TECHNICAL REPORT

Doc.No : 004.2004
Version : 3
Date : 22 Nov 2006

Optical figuring specifications for thin shells to be used in adaptive telescope mirrors

Armando Riccardi
INAF-Osservatorio Astrofisico di Arcetri

Arcetri technical report ID: **004.2004**
ESO doc. ID: **VLT-SPE-OAA-11255-0001**
Issue: **3**
Date: **22 Nov 2006**

Prepared by: Armando Riccardi
(A.Riccardi)

INAF – Osservatorio Astrofisico di Arcetri
Largo E. Fermi, 5 - 50125 Firenze - ITALY
http://www.arcetri.astro.it/adopt

ABSTRACT

The present report describes the guidelines to define the optical figuring specifications for optical manufacturing of thin shells to be used in adaptive optics correctors with force actuators like Deformable Secondary Mirrors (DSM). In particular the numerical example for a thin shell for a VLT DSM is considered in the framework of its straw-man design.

Modification Record

Version	Date	Author	Section/Paragraph affected	Reason/Remarks
DRAFT	20 Sep 2004	Armando Riccardi	All	Draft release of the document
1.0	20 Oct 2004	Armando Riccardi	All	
2.0	05 Mar 2006	Armando Riccardi	Sec.7 Sec.6 Sec.5 Footer	Added missing 2π of eq.22 Fixed PSD units in Fig.1 Add missing D^2 in Eq.20-21 Fixed ZIP code
3.0	22 Nov 2006	Armando Riccardi	Sec.3 Sec.7	Removed double copy of Eq.20. Type error in Eq.24 (removed an exponent 2)

Abbreviations, acronyms and symbols

Symbol	Description
AO	Adaptive Optics
DSM	Deformable Secondary Mirror
FEA	Finite Element Analysis
FPT	Flattening Print-Through
HOP	High Order Polishing
VLT	Very Large Telescope

Contents

1 Introduction

In principle the optical specifications for a thin shell, to be used for a deformable secondary mirror (DSM), can be relaxed considering that actuators can compensate for figuring errors. However the amount of this static error is limited by three main factors:

- the absolute peak force needed to flatten the shell must be limited for power dissipation reasons and to prevent a reduction of the effective actuator force stroke devoted for turbulence correction;
- the optical polishing of the shell at scales shorter than the Nyquist limit of correction (twice the actuator separation) do not have to limit the overall performances of the AO system in best seeing conditions. We will refer to this kind of error as high order polishing (HOP) error;
- the correction of figuring error at scales longer than the Nyquist limit introduces some error at scales shorter then the Nyquist limit as harmonics of the low-order correction. We address this error as flattening print-though (FPT) error. This kind of error does not have to limit the overall performances of the AO system in best seeing conditions.

The previous statements depend on the definition of "performances of the AO system". Hereafter we consider only the unavoidable contribution of fitting error to the residual of the AO correction. From the shell specification point of view this is a conservative (more strict) condition. In this hypothesis the power spectral density (PSD) $\Phi_{AO}(\mathbf{k})$ of the AO residual wavefront correction is given by

$$(1)\quad \Phi_{AO}(\mathbf{k}) = \begin{cases} 0 & \text{if } \mathbf{k} \text{ is inside the Nyquist domain} \\ \Phi_{Turb}(\mathbf{k}) & \text{if } \mathbf{k} \text{ is ouside the Nyquist domain} \end{cases},$$

where $\Phi_{Turb}(\mathbf{k})$ is the power spectrum of the atmospheric wavefront distortions. We define that HOP and FPT errors do not limit the AO performance when their power spectra do not exceed the profile of $\Phi_{AO}(\mathbf{k})$ for any value of the spatial frequency $\mathbf{k}$.

This document provides formulas for the characterization of the above errors/limitations. Moreover those formulas are used to obtain a specification for the optical figuring of the thin shell in the framework of a straw-man design of a DSM.

2 Model definition

Because the framework of this analysis is a straw-man design, a simplified model of the thin shell is considered in order to obtain the required results in terms of analytical functions of the system parameters. We model the shell as:

- an infinite flat plate of constant thickness t;
- a squared grid of force actuators with pitch l.

With the first condition we neglect the effects introduced by the edge and the non-zero curvature of the shell. These effects are beyond the straw-man analysis and have to be evaluated though shell FEA using the final actuator geometry.

Let us consider a surface error $z_0(\mathbf{r})$ to be compensated by the force actuators, where $\mathbf{r}=(x,y)$ is a generic point on the mid-vain plate surface. Let us define $z(\mathbf{r})$ the plate deformation obtained applying the force pattern $f_{n,m}$ at the actuator locations $\mathbf{r}_{n,m}=(x_n,y_m)=(nl,ml)$. The aim of the analysis is to find the deformation $z(\mathbf{r})$ that best fits the figuring error $z_0(\mathbf{r})$, and specify the limits on $z_0(\mathbf{r})$ and $f_{n,m}$ in order to verify the conditions stated in Sec. 1. Because the final figuring error is unknown at this stage, we will specify it in terms of its statistical properties, in particular in terms of its PSD.

3 PSD of residuals after flattening figuring error

In Appendix II it is shown that the PSD $\Phi_z(\mathbf{k})$ of $z(\mathbf{r})$ is given by:

$$\Phi_z(\mathbf{k})=\frac{\sum_{p,q=-\infty}^{+\infty} A_{p,q}\exp(il\mathbf{p}\cdot\mathbf{k})}{D^2k^8}, \quad (2)$$

where $\mathbf{p}=(p,q)$ and the coefficients $A_{p,q}$ are related to the actuator forces $f_{n,m}$ by the relationship

$$A_{p,q}=\lim_{N\to\infty}\frac{1}{(2Nl)^2}\sum_{n,m=-N}^{+N} f_{n,m}\,f_{n+p,m+q}\,. \quad (3)$$

Because the sum in Eq. (2) represents a periodic function with period $k_0=2\pi/l$ in the spatial frequency domain, it is possible to match the PSD of the shell deformation $z(\mathbf{r})$ to a generic PSD of figuring error $z_0(\mathbf{r})$ (i.e. fit z to z_0) only on the central square patch $W_{0,0}$ (Nyquist patch) defined by

$$W_{0,0}:|k_x|<\frac{1}{2}k_0 \text{ and } |k_y|<\frac{1}{2}k_0\,. \quad (4)$$

The fitting is possible by letting in the Nyquist patch:

$$D^2k^8\Phi_{z0}(\mathbf{k})=\sum_{p,q=-\infty}^{+\infty} A_{p,q}\exp[il\mathbf{p}\cdot\mathbf{k}] \quad \text{if} \quad \mathbf{k}\in W_{0,0} \quad (5)$$

See Appendix III for a discussion about the behavior of $k^8\Phi_{z0}(\mathbf{k})$ for $k\to 0$. In this conditions the PSD of $z(\mathbf{r})$ becomes

$$\Phi_z(\mathbf{k})=\begin{cases}\Phi_{z0}(\mathbf{k}) & \text{if } \mathbf{k}\in W_{0,0}\\ \dfrac{(\mathbf{k}-k_0\mathbf{p})^8}{k^8}\Phi_{z0}(\mathbf{k}-k_0\mathbf{p}) & \text{if } \mathbf{k}\in W_{p,q}:\ (p,q)\neq(0,0)\end{cases}. \quad (6)$$

where $W_{p,q}$ are square patches of periodicity with latus k_0 in the spatial frequency domain, and they are defined as

$$W_{p,q}:|k_x-pk_0|<\frac{1}{2}k_0 \text{ and } |k_y-qk_0|<\frac{1}{2}k_0\,.$$

When the deformation $z(\mathbf{r})$ is applied to flatten the $z_0(\mathbf{r})$ figuring error, the PSD $\Phi_{z-z0}(\mathbf{k})$ of the residual is given by

$$\Phi_{z-z0}(\mathbf{k})=\Phi_z(\mathbf{k})+\Phi_{z0}(\mathbf{k})-2\Phi_{z,z0}(\mathbf{k}), \quad (7)$$

where $\Phi_{z,z0}(\mathbf{k})$ is the cross-PSD between $z(\mathbf{r})$ and $z_0(\mathbf{r})$. Because the perfect match between $z(\mathbf{r})$ and $z_0(\mathbf{r})$ in $W_{0,0}$ and assuming spectral components of the figuring error inside $W_{0,0}$ uncorrelated with respect to components outside $W_{0,0}$, we have

(8) $$\Phi_{z,z0}(\mathbf{k}) = \begin{cases} \Phi_{z0}(\mathbf{k}) & \text{if } \mathbf{k} \in W_{0,0} \\ 0 & \text{if } \mathbf{k} \notin W_{0,0} \end{cases}.$$

Finally, using Eqs. (6), (7) and (8) we obtain the following expression for the PSD of the residual error after flattening the shell

(9) $$\Phi_{z-z0}(\mathbf{k}) = \begin{cases} 0 & \text{if } \mathbf{k} \in W_{0,0} \\ \Phi_{z0}(\mathbf{k}) + \dfrac{(\mathbf{k}-k_0\mathbf{p})^8}{k^8}\Phi_{z0}(\mathbf{k}-k_0\mathbf{p}) & \text{if } \mathbf{k} \in W_{p,q} : (p,q) \neq (0,0) \end{cases}$$

The first term of the sum outside $W_{0,0}$ represents the HOP error, the second term represents the FPT error. Note that both terms do not depend on the flexural rigidity (i.e. on t^3 and on the choice of the shell material).

4 Specifications in terms of power spectrum of figuring error

To set the condition that HOP does not limit the performance of the AO in best seeing conditions, we have from Eq. (1):

(10) $\Phi_{z0}(\mathbf{k}) \leq \frac{1}{4}\Phi_{Turb}(k)$ outside $W_{0,0}$,

where the factor ¼ takes in account the wavefront to surface conversion of the PSD. For the FPT error we have a similar condition:

(11) $\frac{(\mathbf{k}-k_0\mathbf{p})^8}{k^8}\Phi_{z0}(\mathbf{k}-k_0\mathbf{p}) \leq \frac{1}{4}\Phi_{Turb}(\mathbf{k})$ inside $W_{p,q}$:(p,q)≠(0,0).

Considering the transformation $\mathbf{k}-k_0\mathbf{p} \to \mathbf{k}$, the previous equation can be rewritten as

(12) $\frac{k^8}{(\mathbf{k}+k_0\mathbf{p})^8}\Phi_{z0}(\mathbf{k}) \leq \frac{1}{4}\Phi_{Turb}(\mathbf{k}+k_0\mathbf{p})$ with $\mathbf{k} \in W_{0,0}$ for any $\mathbf{p} \neq (0,0)$,

or better

(13) $\Phi_{z0}(\mathbf{k}) \leq \frac{1}{4}\inf_{\forall \mathbf{p}\neq(0,0)}\left[\frac{(\mathbf{k}+k_0\mathbf{p})^8}{k^8}\Phi_{Turb}(\mathbf{k}+k_0\mathbf{p})\right]$ with $\mathbf{k} \in W_{0,0}$,

Considering that the PSD of the turbulence decreases with $k^{-11/3}$ power law, the previous condition can be rewritten as the simpler, but more conservative, following condition

(14) $\Phi_{z0}(\mathbf{k}) \leq \frac{1}{4}\Phi_{Turb}(k_0-k)\frac{(k_0-k)^8}{k^8}$ with $\mathbf{k} \in W_{0,0}$.

Finally, joining Eq. (10) and (14) we can define an envelope function $\Phi_{z0,env}(k)$ for the figuring error PSD

$$(15)\ \Phi_{z0}(\mathbf{k}) \le \Phi_{z0,env}(k) = \begin{cases} \Phi_{z0,env}(k_L)\left(\dfrac{k_L}{k}\right)^6 & \text{if } k < k_L = \dfrac{2\pi}{L} \\ \dfrac{1}{4}\Phi_{Turb}(k_0 - k)\dfrac{(k_0 - k)^8}{k^8} & \text{if } \mathbf{k} \in W_{0,0} \text{ and } k \ge k_L \\ \dfrac{1}{4}\Phi_{Turb}(k) & \text{if } \mathbf{k} \notin W_{0,0} \end{cases},$$

that gives a specification all over the spatial frequency domain in agreement with the HOP and FPT error conditions of Sec. 1 and low-order behavior stated in Appendix III (with L larger then the diameter of the real shell).
Let's consider for $\Phi_{Turb}(k)$ the Kolmogorov spectrum (see Appendix I):

$$(16)\ \Phi_{Turb}(k) = 0.490\frac{\lambda^2}{k^{11/3}(r_0/c)^{11/3}},$$

where r_0 is the Fried parameter of the best seeing at wavelength λ and c is the optical compression factor between primary mirror and the DSM. The condition on the figuring error stated in Eq. (16) becomes

$$(17)\ \Phi_{z0}(\mathbf{k}) \le \Phi_{z0,env}(k) = \begin{cases} 0.122\dfrac{(k_0 - k_L)^{13/3}}{k_L^2 k^6}\dfrac{\lambda^2}{(r_0/c)^{5/3}} & \text{if } k < k_L = \dfrac{2\pi}{L} \\ 0.122\dfrac{(k_0 - k)^{13/3}}{k^8}\dfrac{\lambda^2}{(r_0/c)^{5/3}} & \text{if } \mathbf{k} \in W_{0,0} \text{ and } k \ge k_L \\ 0.122\dfrac{1}{k^{11/3}}\dfrac{\lambda^2}{(r_0/c)^{5/3}} & \text{if } \mathbf{k} \notin W_{0,0} \end{cases}.$$

5 Specification in terms of flattening peak force

Appendix II reports in Eq. (35) the relation between the actuator rms force σ_f and the PSD of the flattening correction. Using Eqs. (6) and (17), the integral can be computed and gives (with $L \to \infty$)

$$(18)\ .\ \sigma_f \le \left(\frac{l^2}{(2\pi)}\int_{-k_0/2}^{-k_0/2}\int_{-k_0/2}^{-k_0/2} k^8 \Phi_{z0,env}(k)\,\mathrm{d}\mathbf{k}\right)^{1/2} = 7.86\frac{\lambda D}{l^{7/6}(r_0/c)^{5/6}}$$

The rms force depends on the plate thickness and shell materials through the flexural stiffness D (see Appendix II, Eq. (28)).

Hereafter we assume the peak force equal to $4\sigma_f$. In case the peak force would be greater then the allowed maximum force $f_{\max}$ (see first condition of Sec. 1) the profile of $\Phi_{z0,env}(k)$ has to be modified inside $W_{0,0}$ in order to match the condition $4\sigma_f < f_{\max}$.

Instead of simply scaling the PSD of Eq. (17), we choose to change its power low in order to obtain a larger reduction of the force contribution given by the high (more stiff) spatial frequencies. Assuming

(19) $\Phi_{z0,env}(k) = ak^{-9}$ if $\mathbf{k} \in W_{0,0}$ and $k \geq k_L$,

it is possible to find the constant a that satisfies the $4\sigma_f = f_{\max}$ condition (with $L \to \infty$):

(20) $a = 0.111 \dfrac{f_{\max}^2}{D^2 l^3}$

Considering the peak-force limitation, the envelop $\Phi_{z0,env}(k)$ of Eq. (17) can rewritten as

$$(21)\ \Phi_{z0,env}(k) = \begin{cases} \Phi_{z0,env}(k_L)\left(\dfrac{k_L}{k}\right)^6 & \text{if } k < k_L = \dfrac{2\pi}{L} \\ \min\left[0.111 \dfrac{f_{\max}^2}{D^2 l^3}\dfrac{1}{k^9}, 0.122 \dfrac{(k_0 - k)^{13/3}}{k^8}\dfrac{\lambda^2}{(r_0/c)^{5/3}}\right] & \text{if } \mathbf{k} \in W_{0,0} \text{ and } k \geq k_L \\ 0.122 \dfrac{1}{k^{11/3}}\dfrac{\lambda^2}{(r_0/c)^{5/3}} & \text{if } \mathbf{k} \notin W_{0,0} \end{cases}$$

6 VLT DSM numerical case

Considering the VLT DSM case (see Refs. [2] and [3]):

- $r_0(\lambda=500\text{nm})=50$ cm (0.21arcsec seeing)

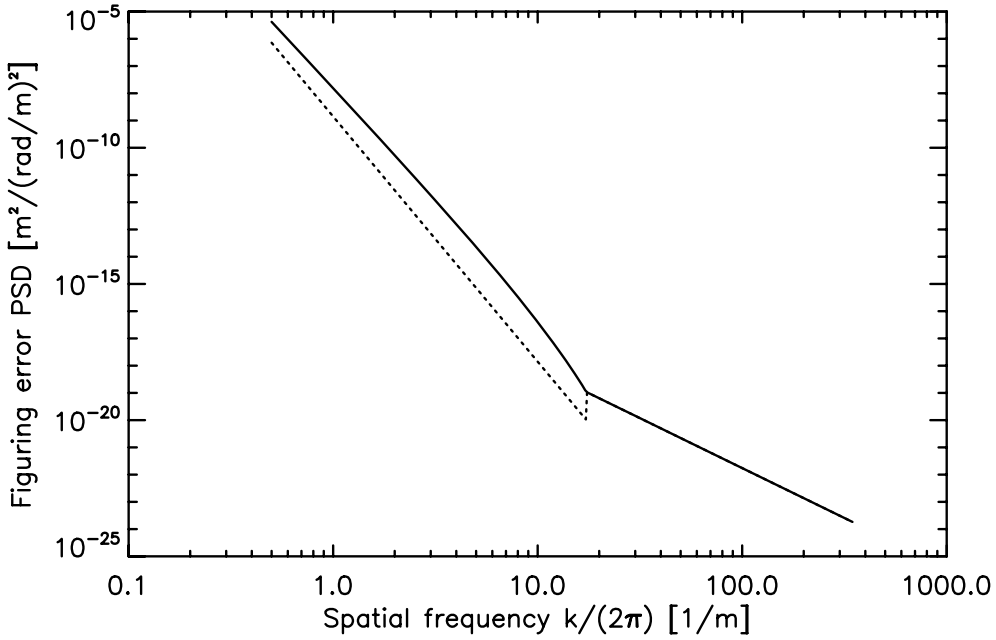

Fig. 1: **Envelope of the figuring error PSD for VLT DSM to avoid that the flattening residuals limit the performance of the AO correction with 0.21arcsec seeing of the PSD of the allowed figuring error. The dashed curve is the PSD envelope taking in account the limitations on the maximum force that can be used to flatten the figuring error.**

- l = 28.9mm
- t = 1.8mm
- shell material: Zerodur
- M1 optical diameter: 8.115 m
- M2 optical diameter: 1.116 m (c=7.27)
- Maximum flattening force f_{max}=0.1N (1/10 of peak force)

The envelope function $\Phi_{z0,env}(k)$ of the figuring error PSD is shown in Fig. 1.

7 Specification in terms of cumulative rms of figuring error

Most of commercial interferometers (like Wyko or Zygo) used for testing optical surfaces are provided of analysis software that computes rms error in a given range of spatial scales. In our case the surface error rms $\sigma_e(d)$ that is generated at scales shorter then a given threshold d (i.e. spatial frequencies larger then or equal to $2\pi/d$) is defined as

(22) $$\sigma_e^2(d) = \frac{1}{(2\pi)^2} \int_{2\pi/d}^{\infty} \Phi_{z0}(k) 2\pi k \mathrm{d}k$$

The condition $\Phi_{z0}(k) \le \Phi_{z0,env}(k)$ can be rewritten in terms of $\sigma_e^2(d)$ and the analogous function

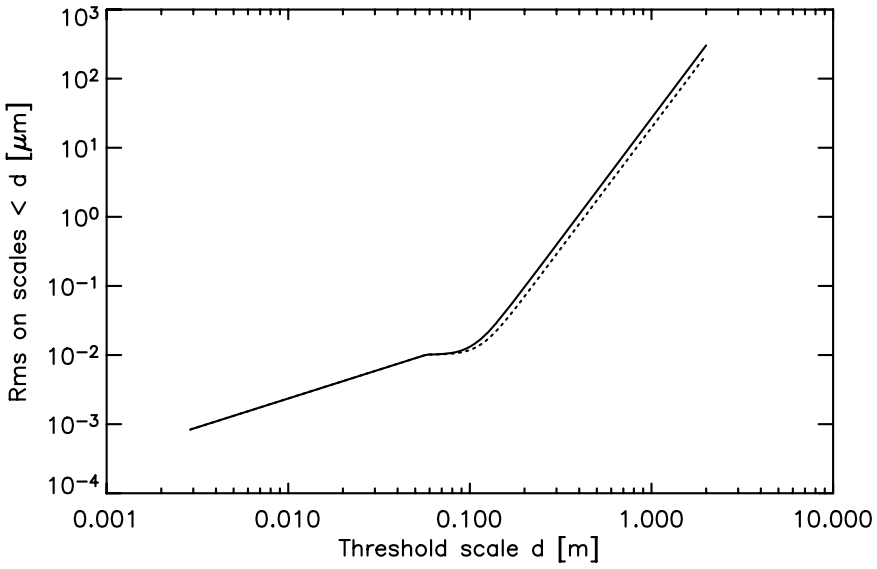

Fig. 2: **Maximum rms figuring error integrated over the range of spatial scales 0÷*d* as a function of *d* for the VLT DSM. The solid and dashed lines represent the 2.0mm and 1.8mm thickness case respectively.**

$\sigma^2_{e,env}(d)$ as

(23) $$\frac{\mathrm{d}\sigma_e^2}{\mathrm{d}d}(d) \le \frac{\mathrm{d}\sigma^2_{e,env}}{\mathrm{d}d}(d)$$

Supposing the peak force limitation as dominant limitation and $d<L$, the integral of Eq. (22) has the following solution:

(24) $$\sigma_e(d) = \begin{cases} 2.15\times10^{-2}\lambda\left(\dfrac{d}{r_0/c}\right)^{5/6} & d \le 2l \\ \left\{3.73\times10^{-9}\dfrac{f^2_{\max}}{D^2 l^3}\left[d^7-(2l)^7\right]+\sigma_e^2(2l)\right\}^{1/2} & d > 2l \end{cases}$$

from which the condition of Eq. (24) can be computed. The plot of $\sigma_e(d)$ for the VLT DSM case is shown in Fig. 2. Numerical values of $\sigma_e(d)$ and $\mathrm{d}\sigma_e^2/\mathrm{d}d$ are reported in Tab. 1.

8 Conclusions

We obtained a specification for the optical quality of a thin shell in terms of the envelope of the figuring error power spectral density (Eq. (21), Fig. 1). We also obtained an alternative specification in terms of maximum rms of figuring error on spatial scales shorter then or equal to a given threshold scale (Eq. (24), Fig. 2) and its derivative with respect to the threshold scale. The last specification is easier to verify because it is related to the output provided by software of commercial optical-test equipment.

The above specifications are obtained considering a limit in the maximum force available for flattening the shell and a minor impact of the residual flattening error on the adaptive optics performances even in good seeing conditions.

Scale range 0÷d	t = 1.6mm		t = 1.8		t = 2.0	
	$\sigma(d)$	$d\sigma^2(d)/dd$	$\sigma(d)$	$d\sigma^2(d)/dd$	$\sigma(D)$	$d\sigma^2(d)/dd$
[mm]	[nm]	[nm^2/mm]	[nm]	[nm^2/mm]	[nm]	[nm^2/mm]
0÷20	3.8	1.2	3.8	1.2	3.8	1.2
0÷40	6.8	1.9	6.8	1.9	6.8	1.9
0÷60	9.3	0.47	9.3	0.23	9.3	0.12
0÷80	11	2.7	10	1.3	9.7	0.70
0÷100	15	10	13	5.0	11	2.7
0÷120	25	30	18	15	15	8.0
0÷140	40	77	29	38	22	20
0÷160	63	170	45	84	33	45
0÷180	95	350	67	170	49	91
0÷200	140	650	96	320	70	170
0÷240	260	1.9×10^3	180	960	130	510
0÷280	440	4.9×10^3	310	2.4×10^3	230	1.3×10^3
0÷320	710	11×10^3	500	5.4×10^3	360	2.9×10^3
0÷360	1.1×10^3	22×10^3	750	11×10^3	550	5.8×10^3
0÷400	1.5×10^3	42×10^3	1.1×10^3	21×10^3	790	11×10^3
0÷450	2.3×10^3	84×10^3	1.6×10^3	42×10^3	1.2×10^3	22×10^3
0÷500	3.4×10^3	160×10^3	2.4×10^3	78×10^3	1.7×10^3	42×10^3
0÷550	4.7×10^3	280×10^3	3.3×10^3	140×10^3	2.4×10^3	74×10^3
0÷600	6.4×10^3	470×10^3	4.5×10^3	230×10^3	3.3×10^3	120×10^3
0÷700	11×10^3	1.2×10^6	7.7×10^3	590×10^3	5.6×10^3	310×10^3
0÷800	17×10^3	2.7×10^6	12×10^3	1.3×10^6	8.9×10^3	700×10^3
0÷900	26×10^3	5.4×10^6	19×10^3	2.7×10^6	13×10^3	1.4×10^6
0÷1000	38×10^3	10×10^6	27×10^3	5.0×10^6	20×10^3	2.7×10^6
0÷1100	53×10^3	18×10^6	37×10^3	8.9×10^6	27×10^3	4.7×10^6

Tab. 1: **$\sigma(d)$: max allowed value of surface error rms within scale range 0÷d.**
$d\sigma^2(d)/dd$: max allowed value of derivative of the surface error variance ($\sigma^2(d)$)

Appendix I Fourier transform definition

In the present work we use the following definition for the Fourier transform $G(\mathbf{k})$ of a 2D-function $g(\mathbf{r})$ as:

(25) $G(\mathbf{k}) = \iint g(\mathbf{r}) \exp(-i\mathbf{k}\cdot\mathbf{r}) d\mathbf{r}$,

(26) $g(\mathbf{r}) = \frac{1}{(2\pi)^2} \iint G(\mathbf{k}) \exp(i\mathbf{k}\cdot\mathbf{r}) d\mathbf{k}$.

Appendix II PSD of a thin-plate deformation

The equation relating the plate deformation $z(\mathbf{r})$ with respect to the pressure pattern $P(\mathbf{r})$ is given by

(27) $D\nabla^4 z(\mathbf{r}) = P(\mathbf{r})$,

where D is the flexural rigidity. D is given by

(28) $D = \frac{Et^3}{12(1-\sigma^2)}$,

where t is the thickness of the plate, E is the Young modulus and σ is the Poisson's ratio of the shell material. The pressure pattern given by the grid of localized force actuators can be written as a sum of Dirac-delta functions

(29) $P(\mathbf{r}) = \sum_{n,m=-\infty}^{+\infty} f_{n,m}\delta(\mathbf{r}-\mathbf{r}_{n,m})$,

where $f_{n,m}$ is the force applied by the actuator in the location $\mathbf{r}_{n,m}=(x_n,y_m)=(nl,ml)$. From Eq. (27) the relationship between the PSD $\Phi_z(\mathbf{k})$ of the plate deformation $z(\mathbf{r})$ and the PDS $\Phi_P(\mathbf{k})$ of the pressure pattern $P(\mathbf{r})$ is given by

(30) $D^2k^8\Phi_z(\mathbf{k}) = \Phi_P(\mathbf{k})$.

The PSD of the pressure pattern of Eq. (29) is given by[1]:

(31) $\Phi_P(\mathbf{k}) = \sum_{p,q=-\infty}^{+\infty} A_{p,q} \exp(il\mathbf{p}\cdot\mathbf{k})$,

where $\mathbf{p}=(p,q)$ and

(32) $A_{p,q} = \lim_{N\to\infty} \frac{1}{(2Nl)^2} \sum_{n,m=-N}^{+N} f_{n,m} f_{n+p,m+q}$.

Even if the user can choose an arbitrary pattern of forces $f_{n,m}$, the power spectrum of pressure is periodic in the spatial frequency domain over square patches with latus $k_0=2\pi/l$. That is a consequence of the finite sampling l of actuator grid.

From Eqs. (30) and (31) the PSD of the shell deformation $\Phi_z(\mathbf{k})$ has the form:

(33) $\Phi_z(\mathbf{k}) = \frac{\sum_{p,q=-\infty}^{+\infty} A_{p,q} \exp(il\mathbf{p}\cdot\mathbf{k})}{D^2k^8}$.

In particular $A_{0,0}$ is related to the rms σ_f of the actuator forces as follows:

(34) $\sigma_f^2 = \lim_{N\to\infty} \frac{1}{(2N)^2} \sum_{n,m=-N}^{+N} f_{n,m}^2 = l^2 A_{0,0}$.

From Eq. (31) $A_{0,0}$ represents also the "piston" term of the Fourier series of $\Phi_P(\mathbf{k})$ in the Nyquist patch $W_{0,0}$ (defined as $|k_x| < k_0/2$ and $|k_y| < k_0/2$), then, considering Eqs. (30) and (34), we have

(35) $\sigma_f^2 = l^2 \frac{1}{k_0^2} \iint_{W_{0,0}} \Phi_P(\mathbf{k}) \mathrm{d}\mathbf{k} = \frac{l^4}{(2\pi)^2} \iint_{W_{0,0}} k^8 \Phi_z(\mathbf{k}) \mathrm{d}\mathbf{k}$

Appendix III Constrains on PSDs due to rigid body motions

Using Eq. (27) and (29), the Fourier transform $\tilde{z}(\mathbf{k})$ of the shell deformation $z(\mathbf{r})$ is given by

(36) $Dk^4 \tilde{z}(\mathbf{k}) = \sum_{n,m=-\infty}^{+\infty} f_{n,m} \exp(i\mathbf{r}_{n,m} \cdot \mathbf{k})$

Considering Eq. (36) and the condition that static equilibrium requires that the sum of forces and torques are zero, we can write:

(37) $D \lim_{\mathbf{k}\to 0} k^4 \tilde{z}(\mathbf{k}) = \sum_{n,m=-\infty}^{+\infty} f_{n,m} = 0$

(38) $D \lim_{\mathbf{k}\to 0} \nabla\left[k^4 \tilde{z}(\mathbf{k})\right] = i \sum_{n,m=-\infty}^{+\infty} f_{n,m} \mathbf{r}_{n,m} = 0$

Assuming $\tilde{z}(\mathbf{k}) \propto k^\alpha$ for $\mathbf{k} \to 0$, Eqs. (37) and (38) state the $\alpha > -3$ condition on $\tilde{z}(\mathbf{k})$. A similar condition can be given for $\Phi_z(\mathbf{k})$ as

(39) $\Phi_z(\mathbf{k}) \propto k^{2\alpha} = k^\beta$ with $\beta > -6$

References

[1] A. Papoulis, "The Fourier integral and its applications", McGraw-Hill, 1962, Pag. 249
[2] VLT-TRE-ADS-14690-0001, Issue B, 30 Sep 2004
[3] VLT-TRE-ESO-10000-526, Issue 1.B, 24 Feb 1995